

# PROCEEDINGS OF SPIE

[SPIDigitalLibrary.org/conference-proceedings-of-spie](https://spiedigitallibrary.org/conference-proceedings-of-spie)

## Design considerations of the AO module for the Gemini South multiconjugate adaptive optics system

Eric James, Corinne Boyer, Richard A. Buchroeder, Brent L. Ellerbroek, Mark R. Hunten

Eric James, Corinne Boyer, Richard A. Buchroeder, Brent L. Ellerbroek, Mark R. Hunten, "Design considerations of the AO module for the Gemini South multiconjugate adaptive optics system," Proc. SPIE 4839, Adaptive Optical System Technologies II, (7 February 2003); doi: 10.1117/12.457082

**SPIE.**

Event: Astronomical Telescopes and Instrumentation, 2002, Waikoloa, Hawai'i, United States

# Design considerations of the AO module for the Gemini South multi-conjugate adaptive optics system

E. James<sup>a</sup>, C. Boyer<sup>a</sup>, R. A. Buchroeder<sup>b</sup>, B.L. Ellerbroek<sup>a</sup>, M. Hunten<sup>a</sup>

<sup>a</sup>Gemini Observatory, 670 N. A'ohoku Pl., Hilo, HI 96720; <sup>b</sup>Optical Design Service, 8 S. Bella Vista Drive, Tucson, Arizona 85745

## ABSTRACT

The adaptive optics system for the Gemini South telescope, currently in the design phase, consists of several major subsystem. The largest subsystem, called the AO module, contains most of the optics and electronics and is mounted on one of the Cassegrain instrument ports. The initial system will be a conventional laser guide star AO system, but the plan is to eventually expand it to a multi-conjugate system. The system is being designed to readily add the components necessary to upgrade to a multi-conjugate system. This paper describes the design challenges encountered and solutions that were derived for the AO module design. The complexity of the multi-conjugate version is illustrated, including optical, mechanical, electronic and controls issues.

Key words: Multi-conjugate adaptive optics, laser guide stars, adaptive optical systems

## 1. INTRODUCTION

The Adaptive Optics Module (AOM) includes all of the optics, sensors, and electronics needed to compensate the input f/16 science beam and relay it to a science instrument at f/33. These components include the principal elements of the real-time Multi-Conjugate Adaptive Optics (MCAO) control loop, namely 3 deformable mirrors, a tip/tilt mirror, 5 higher-order LGS wave front sensors, 3 tip/tilt NGS wave front sensors, and the real-time control electronics. The AOM is mounted to the Gemini Instrument Support Structure (ISS).

The Adaptive optics module has three independently mounted sections. The center bay is for the optics bench, the two outer bays are for the electronics enclosures. All three bays are mounted, one at a time, onto the ISS.

Electronics Enclosures

Optical Bench

Instrument Support Structure

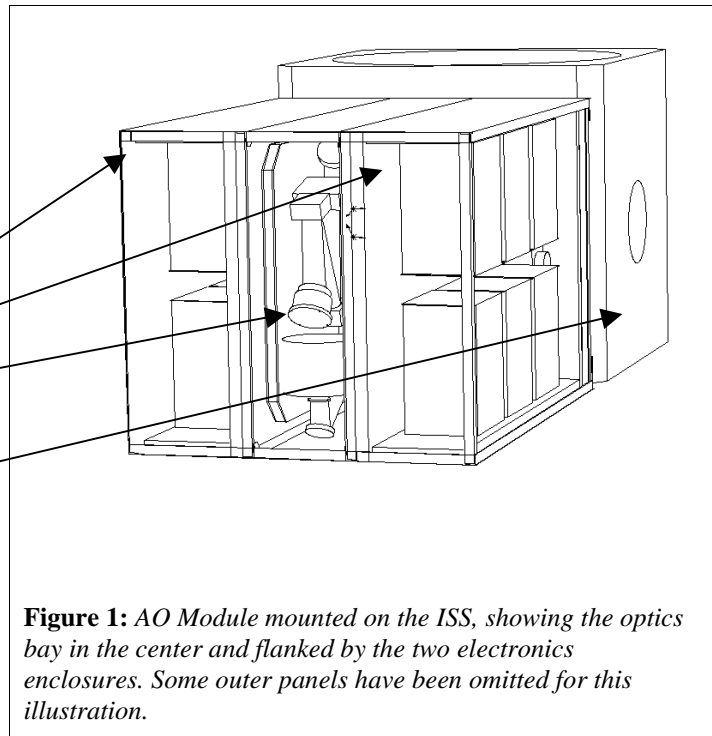


**Figure 1:** AO Module mounted on the ISS, showing the optics bay in the center and flanked by the two electronics enclosures. Some outer panels have been omitted for this illustration.

## 2. OPTICAL BENCH

The Optical Bench consists of the opto-mechanical components of the AOM and the associated sensors,

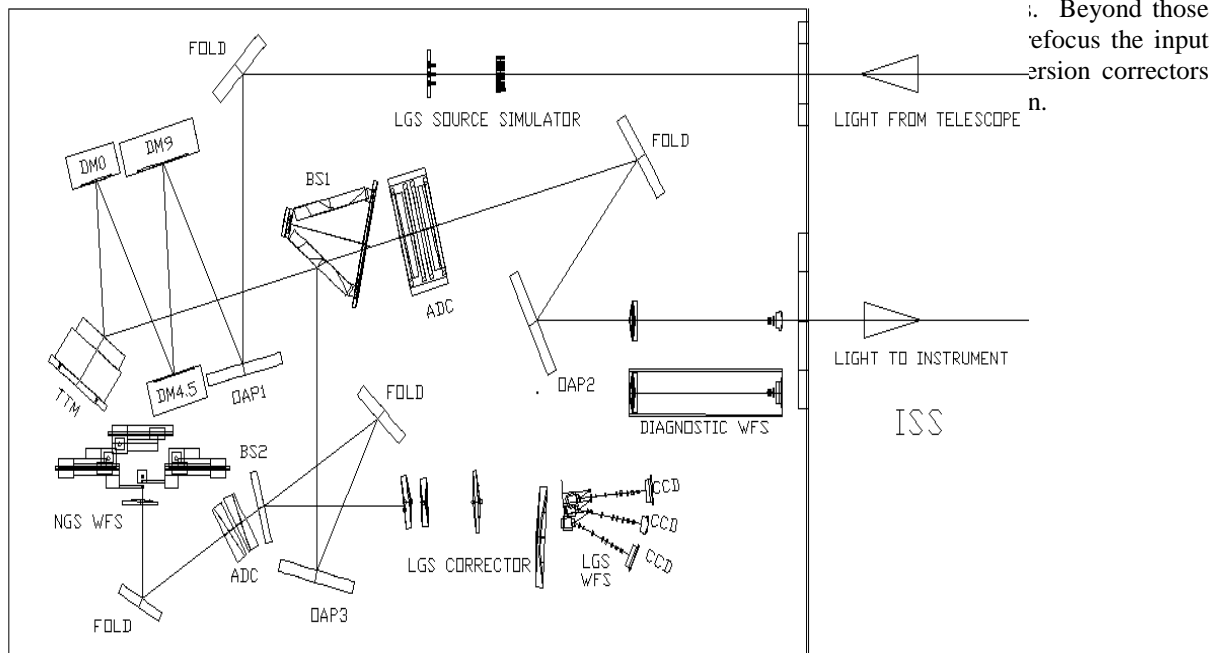


**Figure 2:** AO Bench

- Simulated natural- and laser guide stars located at the Cassegrain focus near the entrance of the AOM. These simulated guide stars are used for (i) verification of optical alignment between AOM and science instruments, (ii) PSF and field distortion calibration, (iii) measurement of DM influence functions and DM-to-WFS alignment, and (iv) closed-loop tests of the MCAO control loop.
- A higher-order WFS located in the output science path. This sensor patrols the 1 arc minute radius field, and is used for diagnostic wave front measurements with the NGS source simulator. These measurements provide an end-to-end evaluation of AO module optical performance, and they are used as input to a “tomographic” wave front reconstruction algorithm to adjust the DM actuator commands and minimize the field-averaged wave front errors in the science path. This sensor in effect substitutes for the “DM interferometer” found in several existing AO systems.

### 2.1. Optical design

The complete optical design of the AO module consists of several sub-designs that serve joint or individual tasks. The Science Path through the module is nearly diffraction limited for the visible spectrum, and fully so for the infrared. The service paths that feed NGS and LGS beams to their respective detectors are likewise nearly diffraction-limited. Special requirements beyond normal resolving power, such as precise mapping of a deformable mirror onto Shack-Hartmann planes, are also addressed and optimized.

### 2.1.1. Design requirements

Top-level optical design requirements for the AO Module are summarized in Table 1. Performance estimates for the current design are *italicized*. The estimated science path wave front error due to flexure at 45 degrees is somewhat larger than the requirement, but this is a preliminary worst-case estimate before any optimization of the mechanical design. The predicted wave front errors in the NGS and LGS WFS paths are within their requirements under the assumption that most of these errors are relatively low order (100 nm RMS coma, for example, corresponds to peak wave front tilts of about 0.1 arc sec). Optical transmittance estimates for the LGS and NGS WFS paths are somewhat below requirements, and the new values have been used to update laser power requirements and NGS magnitude limits. Preliminary estimates for pupil imaging are generally consistent with the requirements, and the values for DM-to-WFS misregistration have been used in detailed simulations to assess the impact upon closed-loop AO performance. The requirements for atmospheric dispersion correction have been easily met.

Parameter	Science Path	NGS WFS Path	LGS WFS Path
Spectral passband, $\mu\text{m}$	<b>0.85-2.5</b>	<b>0.5-0.85</b>	0.589
Field-of-view radius, arc min	1	1	1 (width of square FOV) 90—200 km range
Wave front quality	60 nm RMS uncorrectable and non-common path errors ( <i>59 nm at zenith; 96 at 45 degrees</i> )	0.15 arc sec RMS spot size ( <i>120 nm RMS WFE</i> )	Peak subaperture tilts less than 0.1 arc sec ( <i>102 nm RMS WFE</i> )
Optical transmittance	0.75 ( <i>0.74 at 1.0 micron; 0.80 at 1.65; 0.82 at 2.2</i> )	0.7 ( <i>0.46 at 0.5 micron; 0.69 at 0.7</i> )	0.7 ( <i>0.65</i> )
Pupil imaging	Worst case pupil motion of 3% on instrument cold stop ( <i>2% RMS</i> )	NA	Worst case WFS-to-DM misregistration 10% of a subaperture width ( <i>6.4% RMS</i> )
Emissivity	19%	NA	NA
Atmospheric dispersion at 45 degrees, arc sec	0.007 for 0.85+/-0.07 $\mu\text{m}$ ( <i>0.002</i> ) 0.010 for 1.25+/-0.1 $\mu\text{m}$ ( <i>0.0039</i> ) 0.013 for 1.65+/-0.1 $\mu\text{m}$ ( <i>0.0019</i> ) 0.018 for 2.20+/-0.2 $\mu\text{m}$ ( <i>0.0023</i> )	0.05	NA

**Table 1: AO Module Optical Design Requirements**

Current performance estimates are *italicized*.

### 2.1.2. The Gemini telescope

The Gemini South 8M telescope is a Ritchey-Chretien “Cassegrain” (coma-free field, residual astigmatism and field curvature) with its aperture stop at the secondary mirror. Its nominal focal length is 128M, clear aperture 7.9M, producing an  $f/16.2$  focus. Since the stop is on the secondary mirror, the distance to focus equals the distance from the exit pupil, 16.549M. With the AO fold mirror inserted, this image plane is located approximately 0.7 meters within the AO module. The image plane for a 2 arc-minute diameter field is 74.47mm in diameter.

### 2.1.3. Science path

The layout of the AO Module science path is shown in Fig. 3, with an on-axis beam. This optical relay changes the focal length to 262.2M,  $f/33.2$ , producing a flat, unvignetted image 152.4mm in diameter, located in the same position as the original Cassegrain focal plane, and with the same exit pupil distance, 16.5M forward of the image. The MCAO focal plane is perpendicular to the apparent optical axis, is diffraction limited, with mapping distortion less than 2% over the field of view. All optical elements have significantly over-sized clear apertures to facilitate component fabrication and to relax non-critical alignment tolerances, ensuring that the transmitted field of view is unvignetted over a field at least 2 arc-minutes in diameter.

The design contains two off-axis paraboloids (OAP's) enclosing three deformable mirrors, a fast tip-tilt mirror (TTM), a beamsplitter that transmits the science path and reflects light to controlling wave front sensors, a two-group atmospheric dispersion corrector (ADC), plus two folding mirrors as required to package the optics.

The two OAP's, designated OAP1 and OAP2, form a finite conjugate relay with collimated light separating them. DM0 is placed at the image of the telescope's secondary mirror (the telescope's aperture stop) formed by OAP1, while OAP2 is separated from DM0 so that the exit pupil distance becomes the same as that of the telescope alone. Because the entrance pupil of this system is nearly telecentric, all principal rays pass through the center of DM0. A paraboloid actually has two foci, one of which is at infinity, and any principal ray that passes through such a focus results in an image free of astigmatism. The mirrors are disposed so that OAP2 cancels coma from OAP1 (as in a Mersenne telescope), and of course there is no spherical aberration. The relay is then tipped about the front focus to provide an output image perpendicular to the central ray, which becomes the apparent optical axis. An additional benefit of using OAPs is that the mapping error is under 2%, something not characteristic of unobstructed reflective designs. Attempts to replace the OAPs with cheaper toroidal mirrors result in serious mapping distortions. Figure 4 and Figure 5 illustrate the H band performance of the science path optical design, which is fully diffraction limited over the full 2 arc minute diameter field of view.

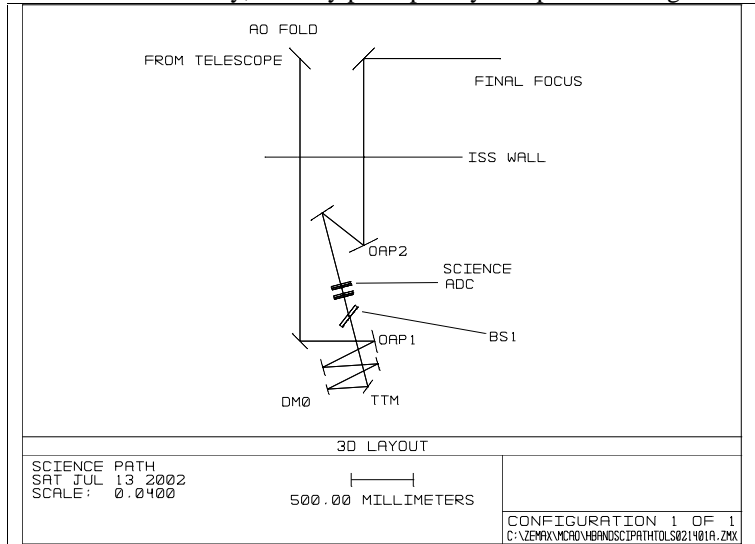
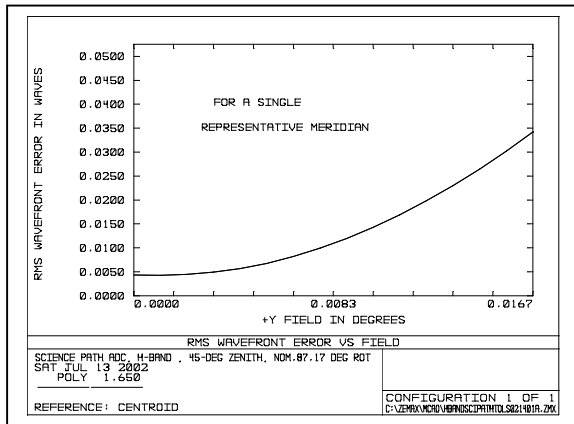


Figure 3: AO Module Science Path



2.1.4. Natural guide star path

Figure 4: H-band RMS wave front error vs. field distance off-axis, for a representative meridian (upper field of view). Zenith Angle = 45 degrees, with ADC in operation to correct atmospheric dispersion.

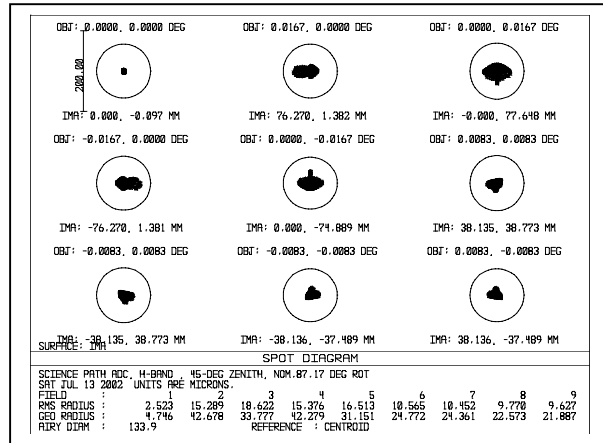


Figure 5: Geometrical spot diagram showing H-band (1.55 – 1.75 microns) image quality over the two arc minute diameter field. Circles show the diameter of Airy Disc, indicating diffraction-limited performance. Zenith angle = 45 degrees, with ADC in operation to correct atmospheric dispersion.

The NGS path is shown in figure 6 with the principal rays.

The incident NGS beam is reflected from BS1 (which transmits the Science Path light), recollimated by OAP3, folded with a flat mirror, transmitted through BS2 (which has a Rugate or similar notch coating to reflect the sodium laser at 589nm), transmitted through an ADC made from anomalous dispersion optical glass, reflected with a fold flat, and transmitted through an aspheric field corrector lens before reaching the detector plane. OAP3 is a duplicate of OAP1.

Used in a converging beam, BS2 introduces ‘prismatic’ aberrations, which we mitigate with a weak

wedge angle and a cylindrical curve on its outgoing face. Along with the ADCs, a decentered aspheric field lens provides wide-field, diffraction-limited imagery over the full bandwidth and full 2 arc-minute field diameter. BS2 is made from fused silica for strength and ease of manufacture, although it no longer needs to be water-free.

Whereas the ADC doublet prisms for the science path are identical because the axial beam is collimated, mechanical and optical advantages result from using different prisms in the NGS path’s converging beam. Two reasonably durable anomalous dispersion glasses were chosen from the Schott glass catalog and paired in doublets that counter-rotate symmetrically (not obligatory, but this simplifies the mechanisms). This approach obtains uniform image quality from 500 nm to 850 nm, and minimizes image “runout.”The image center runs out by about a millimeter as the zenith angle rises to 45-degrees. The mapping distortion of the image also changes, so that a calibration scheme will be necessary to know where the star images are actually located in object space.

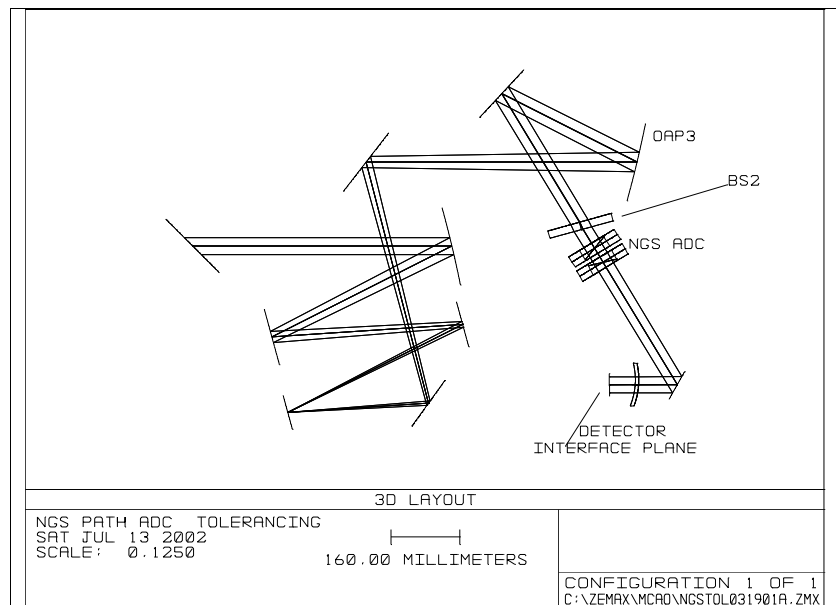


**Figure 6:** NGS Path Optical Layout

### 2.1.5. LGS path

The LGS path is the most challenging. Five laser guide stars are symmetrically arranged in the field of view, one along the “axis”, the other four at angular distances of 42.5 arc-second at the corners of a box with its base parallel to the horizon.

Because the range to the laser guide stars varies between 90 to 200 km, their image locations differ from the Science Path focal point by as much as 184 mm, and by 102 mm from each other. Since these objects are relatively near, rather than at infinity, the telescope introduces small amounts of spherical aberration and coma. More importantly, the reflective relay composed of the two OAP’s shows significantly different aberrations according to the conjugates at which it works, and its magnification changes slightly with LGS range since it is a finite-conjugate relay whose object distance is variable. This causes a change in LGS plate scale, a change in exit pupil distance, a changing location of the image plane, and an unsymmetrical set of aberrations that are ever changing. A means must be found to maintain the locations of both the pupil and image planes, and compensate the aberrations in both of these planes to the requirements indicated in Table 1 .

### 2.1.5.1. LGS path optical layout

The LGS path is illustrated in Figure 7. Laser light at 589 nm is reflected by BS2 at approximately  $f/16$ , and intercepted by a four-element “zoom” system made of BK7 glass lenses, V-coated for high transmission. This zoom system keeps images of laser guide stars, that may reside at slant ranges between 90 and 200km, fixed at a single image distance, at a single plate scale, and makes the principal rays telecentric for convenience in forming images of the pupil on the Shack-Hartmann lenslet arrays. Without the zoom, the images of the laser guide stars would move around as much as 184 mm from the cassegrain focus. Details of the zoom are suggested by Figure 8, which shows the two zooming elements in positions for ranges between 90 and 200km.

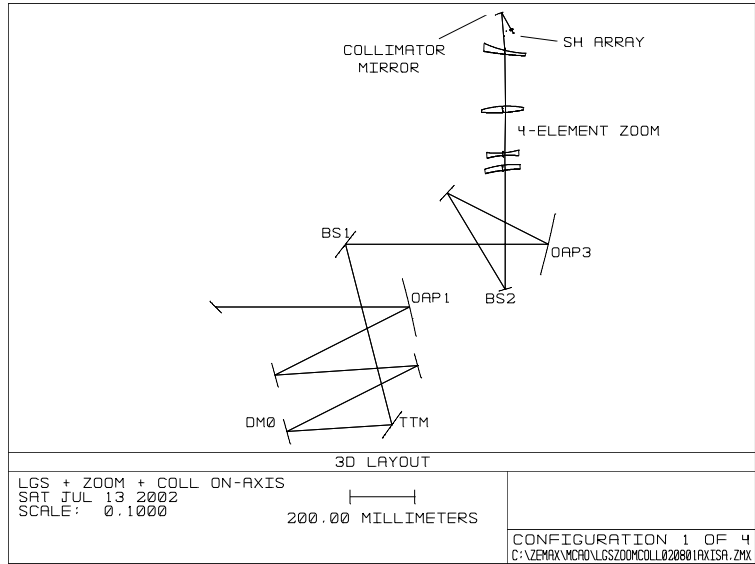


Figure 7: Optical layout of LGS path

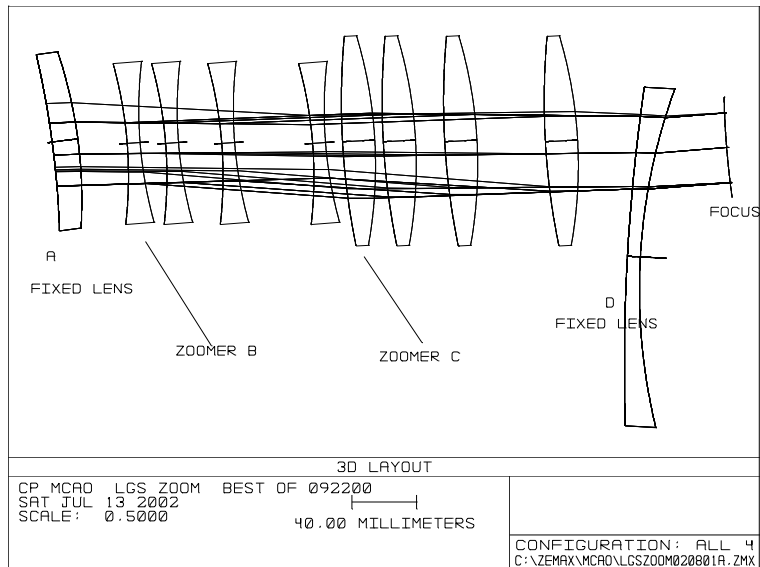


Figure 8: Motion of the zoom group for LGS ranges between 90 and 200 km.

### 2.1.5.2. Collimator to Shack-Hartmann array

Following the focus of the LGS zoom system will be five “magnification correctors” and five “collimator” mirrors, each followed by a folding flat mirror and a cylindrical afocal attachment to restore the obliquely viewed deformable mirrors to circular shape in the pupil which is imaged on the Shack-Hartmann lenslet arrays.

Because the guide stars are located at the four corners of a square aligned with the horizon, with one additional star in the middle, symmetry requires only 3 distinct collimator designs.

The Axial Collimator unit is shown in Figure 9.

The “magnification corrector” is a symmetrical negative lens made from BK7 glass, serving two useful purposes. First, with a +/- 10mm axial motion, it changes the diameter of the exit pupil, on the SH lens array, by +/- 2.5%, to compensate for accumulated fabrication errors and if needed it can be moved according to guide star range to compensate for slight errors in the Zoom. Secondly, it can be decentered by +/- 1mm to center the pupil on the SH array by +/- 300 microns. Tip of the axis is within acceptable bounds. Changes in both image and pupil aberrations are negligible, including defocus.

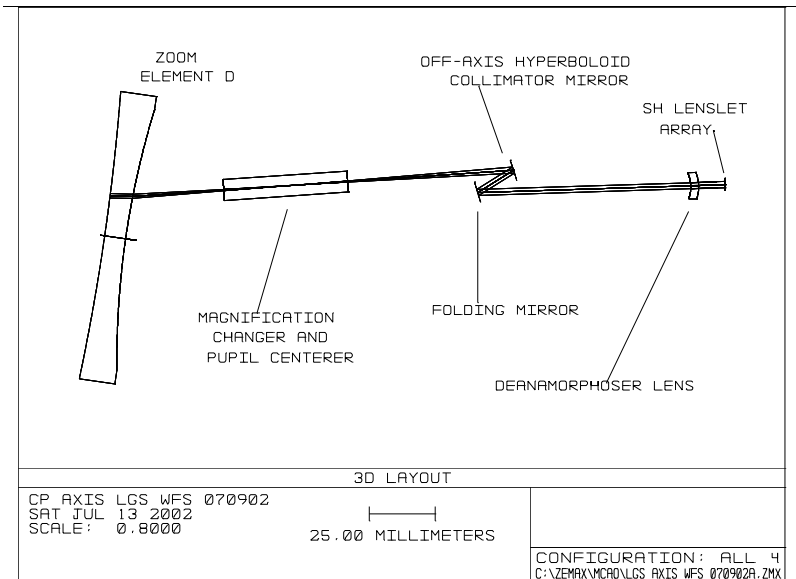


**Figure 9:** Collimator and cylindrical lens to produce circular, non-distorted image of DM0 onto the Shack-Hartmann lens array.

The Collimator is an off-axis mirror, in this case a hyperboloid, whose function is to produce a 4.8 mm diameter collimated beam matched to the size of the SH lenslet array. The pupil will be distorted if we use a simple lens for the collimator, since the image of a tipped DM0 is reflected only once by OAP3. Linear (affine) mapping error, caused by the oblique angles of incidence on DM0, is corrected with the deanamorphoser (cylindrical telescope), which turns the elliptical projection of DM0 back into a circle. Nonlinear warp is corrected by the asphericity of the off-axis collimating mirror.

#### 2.1.5.2.1. LGS Wave Front Detectors

The AO Module includes Shack-Hartmann WFS's for the five laser guide stars. These are implemented with 5 sets of lenslet arrays, optical relays, and CCD arrays. The optical relays are used to obtain the proper spot-to-spot spacing on the CCD array, and are also adjustable in two degrees of freedom to compensate for range-varying aberrations in the LGS path. The present design employs one CCD array per LGS to reduce optical system complexity. The Shack-Hartmann spots will be imaged at the vertices of quad cells composed of 2 by 2 pixels each on the CCD array, with two additional guard rows of pixels between subapertures.

#### 2.1.5.2.2. Shack-Hartmann lenslet array

Each of the SH lenslets, 300 microns on a side, is a high-quality, plano-convex non-binary element. An array has virtually a 100% fill-factor, limited by fractional micron fabrication limits. Optical quality is “diffraction limited,” facilitated by small size and exceedingly relaxed f-numbers. The lenslets, made from fused silica, will be antireflection-coated on both sides. Note that the lenslets have their convex side facing the CCD space; this avoids the multiple reflections that can occur when a flat surface faces a telecentric space.



### 2.1.5.2.3. Shack-Hartmann array to CCD with adjustable relay optics

The wave front incident on the S-H lenslet array varies slightly in focus, size and astigmatism over the Zoom range, causing the centroids of the individual images to displace from those that characterize a flat wave front. The focal plane of the lenslet array is reimaged onto the WFS CCD array pixel size. Since it is not possible to perfectly focus and correct the wave fronts from all five LGS fields at all star ranges using the zoom optics, we are left with small residuals (about 100 nm RMS worst case). The corresponding wave front tilt is an acceptable fraction of the LGS image size, which is estimated to be about 1.2 arc sec FWHM under good seeing conditions.

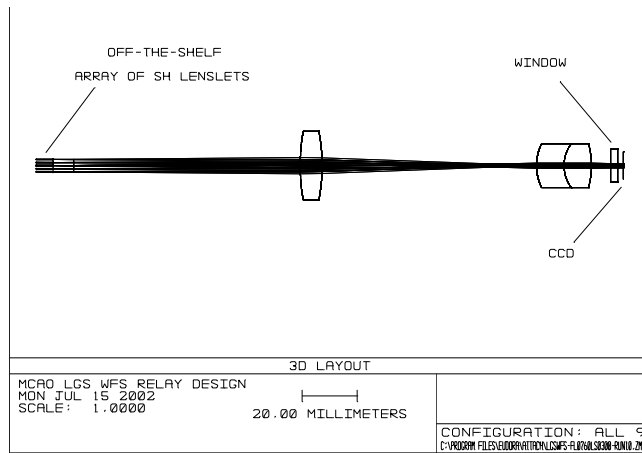


**Figure 10:** LGS WFS SH spot relay with variable magnification and stretch to compensate non-common path errors.

### 2.1.6. Diagnostic wave front sensor

With the aid of star simulator sources located at the front focal plane of MCAO, the quality of the transmitted science path beam can be tested and optimized with a deployable Diagnostic Wave Front Sensor (DWFS). This sensor is inserted into the Science Path following OAP2, and pivots around the exit pupil location that lies some 10 meters to the left of the DWFS. It has a negligible field of view and is pointed toward the simulated NGS star images. The optical layout is shown in Figure 11.

To produce a manageable real image of DM0, we require a large doublet to form an intermediate focus, followed by a small doublet to collimate the light while forming the desired real image, where a small Shack-Hartmann lenslet array of 32 by 32 lenslets is placed. A small cylindrical telescope, the deanamorphoser, is used to rectify the oblique image of tipped DM0. Some residual pupil distortion remains, since DM0's image involves a reflection off just one OAP. This is acceptable, since these wave front measurements are not used in real time and may be post-processed to compensate for the distortion.

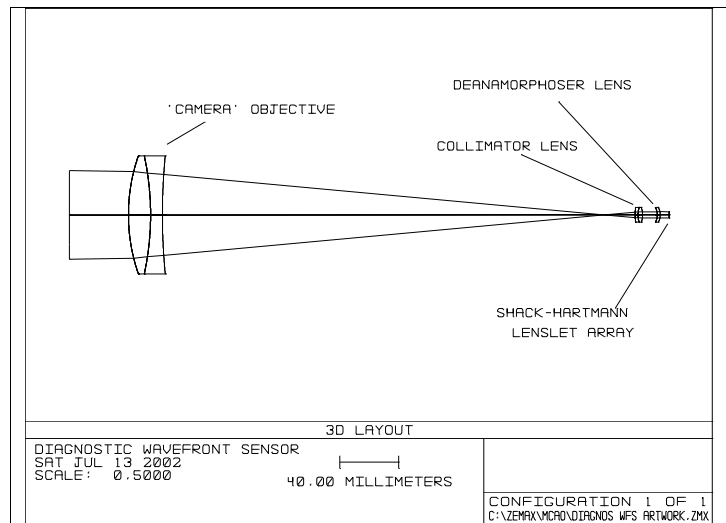


**Figure 11:** Diagnostic Wave Front Sensor optical layout.

## 2.2. Mechanical design

### 2.2.1. Optical bench

The optical bench is based upon a standard optical table system. The table would have custom outer dimensions and perhaps some special mounting features but is otherwise a standard product. The bench has stainless steel face sheets and a honeycomb core. One face sheet has a continuous array of M6 mounting holes at 25 mm centers. All of the optics mounts, cables, ancillary equipment, etc. will be attached with these holes.

The optics are all on a single plane with the incoming beam coming from the telescope via the AO fold mirror in the ISS and the outgoing science beam exiting back into the ISS .

The mechanical design of the AO bench is still in the preliminary design phase. All of the concepts presented here are subject to change as the design progresses.

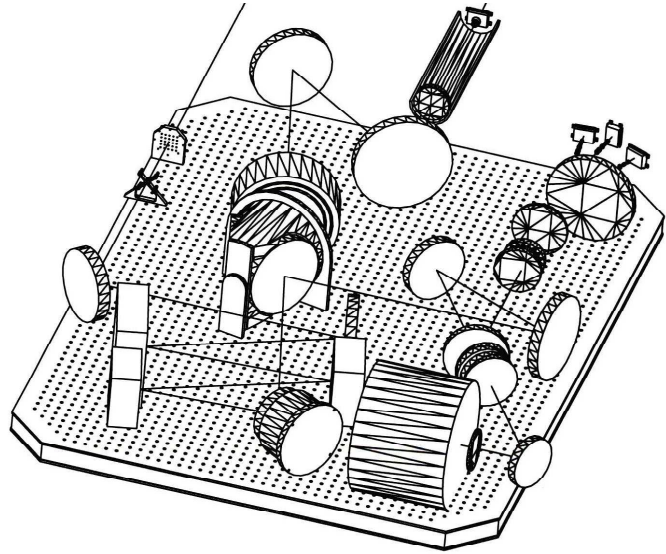


Figure 12: AO bench

### 2.2.2. Bench support frame

A steel frame, stiffened by the optical table and steel shear panels, supports the table. The frame is mounted onto the round mounting pads on the side of the ISS. The mating surface will be made nominally 5 mm shorter than necessary with a nominal 5 mm shim on each mounting surface. The shim can then be made thinner or thicker when the actual mounting position is measured during alignment.

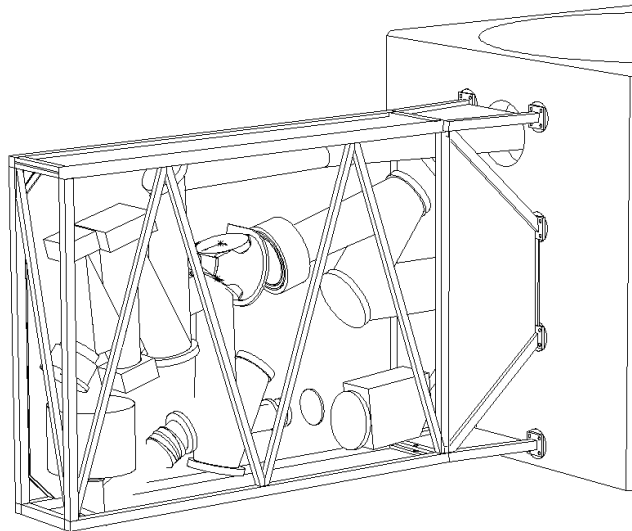


Figure 13: Optical bench with frame mounted on the ISS

### 2.2.3. Subassemblies and components

#### 2.2.3.1. LGS wave front sensor and zoom corrector

The laser guide star wave front sensor has five individual, but basically identical, beams paths – one for each laser guide star. The first set of four optics is the zoom corrector. Each element is tipped and decentered with respect to the optical path. The two outer elements are fixed while the two inner elements translate parallel to the optical path for zoom correction. All five beams go through the same four elements. After the zoom corrector, each of the five beams has its own set of optics. There is one active element in each of the peripheral beams, none in the center beam. The active elements are the long magnification correctors which are continuously decentered to correct for pupil wander induced by the zoom corrector. All of the other elements are fixed after initial alignment.

There are two possible design solutions for packaging the CCDs. One is to use the fold mirror to spread the five paths out so that separate detector assemblies will have sufficient clearance. The other is to mount the individual CCDs onto the same back plane at the correct orientations with respect to each other.

As of yet, no 1  
feasibility. We

ensure mechanical  
ire.

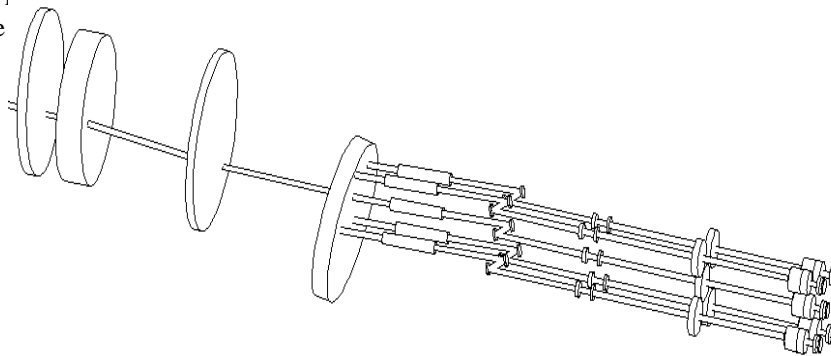


**Figure 14:** Laser Guide Star Wave Front Sensor

#### 2.2.3.2. NGS wave front sensor

The function of the NGS WFS is to patrol a field of 2.2 arc minutes in diameter, and acquire three natural guide stars using three probes. Light is routed by the probes to three quadrant detectors that provide tip-tilt information. The system is required to acquire objects with an accuracy and repeatability of 15 milli arc seconds, and to maintain this accuracy under all orientations. The capture area of each sensor must not be less than 2 arc seconds in diameter.

APDs were chosen for the quadrant detectors. They are preferred over CCDs because of the lower noise, expense, and heat dissipation. The light from each quadrant of a quadrant detector is fed to an APD module via a fiber optic cable with a core diameter of 100 microns. Each module requires a power supply delivering 5 VDC at 2 A. The dark count is as low as 25 counts per second in selected units. The output is in the form of a TTL pulse, 25 nsec wide, for each photon detected, and can drive a 50-ohm load. The peak quantum efficiency is 72% at 700 nm. The signal-to-noise ratio per quadrant is expected to be about 3 for a guide star of 18<sup>th</sup> magnitude.

Light from each guide star is intercepted in the field by a right-angle mirror on the end of a thin probe arm that diverts it into a negative lens on the arm. This lens changes the f-ratio from f/16 to f/53, and relays the light to a collimating lens and a four-sided mirror prism where the stellar image is formed, with a plate scale of 2.0 mm per arc second. Light from the four facets of the mirror prism is reflected to four parabolic mirrors which image the telescope pupil onto the inputs of the four fibers feeding the APDs. The image diameter is 80 microns. This system is similar to the successful tip-tilt guider used in the CFHT SIS instrument.

The capture field of the system is determined by the maximum acceptance angle of the light entering the fibers, and is 2 arc seconds in diameter. The fibers are potted in capillary tubes, and can be aligned in the X, Y and Z directions by adjustment screws to bring the fiber tips and pupil images into alignment.

Each probe assembly is mounted on an X-Y stage adjacent to the patrol area. The optical system is telecentric, so no motion is needed along the optical axis. X and Y slides are sized to allow each probe to access the full field laterally and 75% of the field longitudinally. The slides are actuated by DC motors and ball screws with 400-line rotary encoders. This gives a positioning resolution of 10 milli arc seconds. Ideally the probes should be 120 degrees apart, but space constraints may result in probes being at 0, 90, and 180 degrees.

The twelve optical fibers allow the APD modules to be up to 1 meter from the WFS package. The modules must be mounted on a heat sink to remove the approximately 60W of heat generated, and to keep the operating temperature between 5C and 40C.

### 2.2.3.3. Diagnostic wave front sensor

The diagnostic wave front sensor resides in the science path directly after the second off-axis parabola. It is mounted on a X-Y, tip/tilt stage. The stage allows the wave front sensor to scan the outgoing beam as well as retract from the beam completely. The tip/tilt stage is to maintain accurate pointing as it scans. An additional feature is an internal video camera that can be inserted into the beam ahead of the Shack-Hartman lenses for direct viewing of the output image at video rate.

### 2.2.3.4. Source Simulators

The LGS simulator and NGS simulator are two separate mechanisms but are designed to work both together and independently. Each has a two-position stage for moving it in and out of the beam as well as a continuous Z-motion stage. The NGS simulator is located at the telescope focus while the LGS simulator is located 182.3 mm down stream.

The NGS simulator is fiber fed from a light source located in the electronics enclosure to keep the heat from the lamp out of the optics bay. There is a 5 x 5 array of 4 micron diameter sources in the middle surrounded by a circular array of eight 300 micron sources near the edge of the field (these eight sources are used together with the NGS WFS, and the larger source diameter simulates partial compensation of atmospheric seeing). The sources are in the .50 to 2.5 mm wavelength range. The Z-motion is +/- 1 mm to 40-micron accuracy.

The LGS simulator may use LED's that emit near the .589-micron sodium wavelength. There are five sources arranged in the same X-shaped pattern as the laser guide star constellation. Its Z-motion is 73 mm, corresponding to LGS ranges on the sky from 90 km to 150 km with 40-micron accuracy. The sources are 400 to 600 microns in diameter to simulate extended laser guide stars.

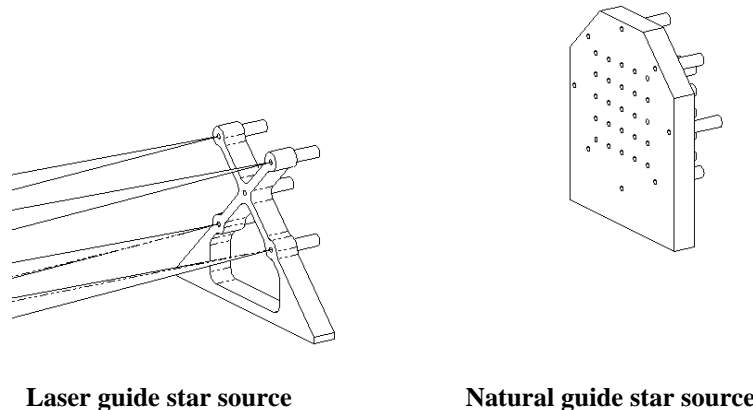


Figure 16: Source simulators

### 2.2.3.5. ADCs

There are two ADCs, one in the science path and one in the NGS path. These are both counter-rotating prisms. The science ADC can be moved out of the beam when observing is done in the L and M bands, where dispersion compensation is unnecessary. The NGS ADC is fixed in position.

### 2.2.3.6. Beam splitter changer

There are two beam splitters. The science path beam splitter can be changed for two different wavelengths. This is accomplished by using a rotating 2-position stage. The second beam splitter splits the LGS and NGS paths and is not changeable.

### 2.2.3.7. Deformable mirrors

Continuous facesheet, stacked actuator deformable mirrors have been assumed due to the order of correction that is required. The three deformable mirrors are optically conjugate to ranges of 0, 4.5, and 9.0 km, with 17, 17, and 9 actuators across the diameter of the collimated 80 mm beam. The resulting inter-actuator spacings are 5.0, 5.0, and 10.0 mm. Each mirror includes rings of guard actuators to provide uniform influence functions for all actively controlled actuators. The sizing for the two mirrors conjugate to 4.5 and 9.0 km must also account for the 2 arc minute diameter field-of-view. These considerations yield the following actuator geometries for each mirror:

- DM0: 241 actively controlled actuators in a 17 by 17 array, within a 21 by 21 array of 349 total actuators. This provides 2 full guard rings around the pupil.
- DM4.5: 352 actively controlled actuators in a 20 by 20 array, within a 24 by 24 array of about 468 total actuators. This provides 2 guard rings for all field points within a *circular* 1.15 arc minute field. For field points at the corners of the fully corrected square 1 arc minute field, the minimum separation between the edge of the beamprint and the outer ring of guard actuators is 1.65 times the inter-actuator spacing. The corresponding value at the edge of the full 2 arc minute field is 0.88.
- DM9: 145 actively controlled actuators in a 13 by 13 array, within a 17 by 17 array of 241 total actuators. This provides 2 full guard rings for all field points in the 2 arc minute field of view.

These mirror sizes have been used for the purposes of packaging the optical design and determining real-time signal processing requirements.

The requirement for peak-to-valley actuator stroke (remaining after DM flattening) is 4 microns. About 65-70 nanometers of RMS stroke will be used to compensate for errors in the AO module. For DM0, the RMS stroke necessary to compensate for atmospheric turbulence under poor (70%) seeing conditions is 500 nm at 45 degrees, and about 615 nm at 60 degrees. The RSS of these values is 504 nm at 45 degrees and 619 nm at 60 degrees, yielding ratios of 7.94-1 and 6.46-1 with the actuator peak-to-valley stroke requirement of 4 microns.

Actuator uniformity and repeatability must be sufficient to allow unobservable mirror modes to be monitored without the use of an interferometer. These modes include piston, waffle, and the high-order modes not actively controlled by the wave front reconstruction algorithm. The requirements on hysteresis are thought to be similar to a conventional AO system, but this effect has not yet been included in simulations.

The baseline mechanical design uses volume estimates supplied by Xinetics. The data is as follows:

9 km DM:	200mm x 200mm x 65 mm,	300 gm.
4.5 km DM:	145 mm x 145 mm x 65 mm,	1500 gm.
0 km DM:	130mm x 130 mm x 65 mm,	1200 gm.

The baseline design also allows room behind the mirror volumes for routing the cables to the many actuators.

The DMs are controlled by the Real Time Computer (RTC) residing in the main thermal enclosures. This is a high bandwidth control system using the 5 CCDs as input from the Laser WFS. The High Voltage Amplifiers (HVA) and electronics for the DMs reside inside the thermal enclosures. The racks for DM0 and DM4.5 require 18U of space each and the rack for DM9 requires 9U of space, not including the power supplies. Power dissipation for these systems is discussed in Appendices P and M. Cabling for the DM's needs to be shielded for noise reduction purposes, and needs to break at the thermal enclosure entrance as well as at the HVA electronics.

### 2.2.3.8. Tip -tilt mirror

The revised AO module optical design now includes a conventional flat tip/tilt mirror at a conjugate range of approximately  $-2$  km. The required clear aperture is 130 mm. The dynamic range requirement is  $\pm 200$  arc sec (TBR), which corresponds to  $\pm 2$  arc seconds on the sky. The closed loop bandwidth requirement is 300 Hz and has been taken from Altair. These values are consistent with the performance of existing mirrors.

Tip/tilt adjustments will slightly alter the DM-to-WFS influence matrix because this mirror is not conjugate to a pupil. The magnitude of these shifts has been estimated from the values for (a) the RMS 1-axis tip/tilt jitter for average seeing, 0.14 arc second, and (b) the RMS 1-axis jitter of 0.13 arc second predicted for windshake under typical conditions. The combined RMS jitter is about 0.2 arc seconds, corresponding to LGS beam print translations of about 0.39, 1.26, and 1.06 per cent of the interactuator spacing on the three deformable mirrors. These translations are acceptable and small compared with the ~6% translations anticipated due to flexure and thermal effects.

This fast Tip/Tilt mirror is also controlled by the RTC using a high bandwidth control system to attain the 300Hz requirement. This will require care with cabling, as high voltage will be required to drive the piezo actuators. Cabling needs to break at the thermal enclosure entrance as well as at the electronics racks.

### 3. ELECTRONICS CABINETS AND ENCLOSURES

#### 3.1. Mechanical design

The baseline design is a welded aluminum frame covered with steel panels. Most components are mounted on a 19-inch rack system, with additional room for some non-rack mounted items. There are 6 racks in each bay, each rack capable of holding a 9U chassis. This gives a total of 12 9U racks.

The electronics enclosures are mounted to the ISS on either side of the optics bay. After the electronics enclosures are mounted, panels are installed between them to enclose the optics bay. Neither the electronics enclosure nor the optics enclosure panels contact the optics bench.

There are doors in the sides that open clamshell style to gain access to the components inside. The racks swing out when the doors are opened to gain better access to the chassis. Access to the optical bay is through a variety of methods. The end panel can be removed for access to the outer region of the electronics bay. Removing the lower panel will gain access to the lower region, including the area containing most of the wave front sensors. The electronic racks on the right electronics enclosures can be pivoted out of the enclosures to reveal the back enclosure surface. Access panels in the surface can then be removed to gain access from the right side of the optical bay. Since the optical table itself prevents access on the left side, there is no access there.

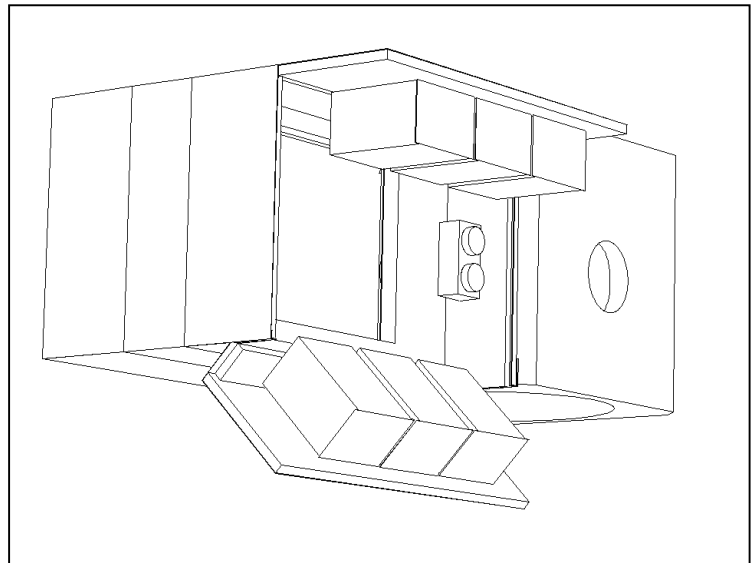


Figure 17: *Electronics enclosure with one bay opened*

#### 3.2. Thermal management

There are two separate electronics enclosures. Each has its own thermal management system. The enclosures are insulated with foam insulation to retard thermal migration into the dome and especially into the optical bay. There is nominally 2 inches of insulation over the entire perimeter with an additional 2 inches at the boundaries to the optics bay. There are water-cooled heat exchangers with a forced air circulation system. Preliminary calculations indicate that the AO module will radiate up to 85 Watts into the dome plus conduct another 11 Watts into the ISS. Of the 85 Watts radiated, 15 Watts are radiated into the optical bay first and then eventually into the dome. The 11 Watts into the ISS is below the 50 Watts allowable, but the 85-Watt radiation load into the dome is over the 50 Watts allowed. These are preliminary calculations based on only a conceptual design. Once a more complete

design is developed, additional work must be done to improve the efficiency of the heat exchange process and reduce the heat losses into the dome to acceptable levels.

#### **4. MASS AND CG BUDGETS**

The latest AO module mass estimate is 971 kg. The requirement is 900 kg. Using aluminum in lieu of steel for the bench material would save approximately 60 kg at the outset. However, since aluminum is not as stiff as steel, this may be more than offset by the additional material required to maintain flexure requirements and deal with larger and dissimilar thermal changes. Some light weighting may be possible but would have to be identified and calculated later in the design process. The 8% by which the mass has exceeded the requirement is not serious as is, but needs to be watched carefully as the design progresses.

#### **ACKNOWLEDGEMENTS**

This work was supported by the Gemini Observatory, which is operated by the Association of Universities for Research in Astronomy, Inc., under a cooperative agreement with the NSF on behalf of the Gemini Partnership: the National Science Foundation (United States), the Particle Physics and Astronomy Research Council (United Kingdom), the National Research Council (Canada), CONICYT (Chile), the Australian Research Council (Australia), CNPq (Brazil), and CONICET (Argentina).

#### **REFERENCES**

1. Brent L. Ellerbroek, et al, *MCAO for Gemini-South*, SPIE conference 4839-07, Kona, 2002
2. MCAO Preliminary Design Review Documentation, Gemini Observatory